Tellus (1989), *41B*, 524–536

Intercomparison of three long-range trajectory models applied to Arctic haze

By JONATHAN D. KAHL, JOYCE M. HARRIS, GARY A. HERBERT, *Geophysical Monitoring for Climatic Change, Air Resources Laboratory, National Oceanic and Atmospheric Administration, 325 Broadway, Boulder, Colorado 80303, USA* and MARVIN P. OLSON, *Atmospheric Environment Service, 4905 Dufferin Street, Downsview, Ontario M3H 5T4, Canada*

(Manuscript received 15 August 1988; in final form 2 December 1988)

ABSTRACT

Three long-range trajectory models which have been applied to Arctic haze problems were compared. These models employ different parameterizations of vertical motions, and are based on different meteorological analyses. Median horizontal displacements between 5-day trajectory endpoints were mostly in the 800–1000 km range. Model sensitivity to the meteorological data was shown to contribute a substantial component to the overall uncertainty. Based on these comparisons, we estimate that the usefulness of trajectory models after 5 days is limited to the identification of distant source regions with horizontal dimensions on the order of 1000 km.

1. Introduction

Trajectory analysis has been successfully applied as an analysis tool for atmospheric transport problems on scales ranging from 100's to 1000's of kilometers. In addition to regional-scale issues such as acid deposition, trajectory analysis has been used in continental- and global-scale problems including Saharan dust transport (Reiff et al., 1986), Asian dust transport to the equatorial Pacific (Merrill et al., 1985), and as will be discussed in this paper, Arctic haze.

A modeled trajectory is an estimate of the transport pathway of an infinitesimally small air parcel. This pathway represents an estimate of the centerline of an advected air mass subject to dispersion in the horizontal and vertical directions. These estimates are based on raw or analyzed data which have spatial and temporal gaps of up to several hundred kilometers and 12 h, respectively. Trajectories corresponding to individual transport events thus provide, at best, an approximate indication of the mean motion of an advected air parcel.

Verification of long-range trajectory models has proven difficult due to the limited availability of observed transport data. Recent papers have reported average horizontal trajectory errors ranging from 140 to 300 km after 24 h, and from 350 to 500 km after 72 h (Kuo et al., 1985; Kahl and Samson, 1986, 1988a; Haagenson et al., 1987; Draxler, 1987). While the magnitude of these errors may be unacceptable in some cases, trajectory models usually provide a useful qualitative estimate of the *general* pathway of an expanding air parcel. Hence, these models enjoy widespread use and acceptance by atmospheric transport researchers.

Trajectory analysis remains the primary means for determining the source regions contributing to the polar-wide air pollution phenomenon known as Arctic haze. First documented in the scientific literature by Mitchell (1957), Arctic haze is characterized by elevated concentrations of gaseous and aerosol contaminants, with peak levels typically occurring in the spring. The northward flux of pollutants to the Arctic is thought to result primarily from meridional transport from industrial sectors of Eurasia.

Numerous studies of Arctic haze transport have relied on trajectory analysis (see the special issues of *Atmospheric Environment*, vol. 15, no. 8, 1981, and vol. 19, no. 12, 1985; and *Geophysical Research Letters*, vol. 11, no. 5, 1984). Because haze events often involve transit times of a week or longer, and since much of the transport occurs above the planetary boundary layer, transport to the Arctic is thought to be nearly adiabatic (Carlson, 1981; Iversen, 1984). Nevertheless, several types of trajectory techniques, including isobaric models, have been used in Arctic haze research with apparent success.

The purpose of this paper is to compare three trajectory models which have been applied to Arctic haze problems and published in the recent literature. Using selected cases corresponding to aircraft measurements of Arctic haze constituents, we address the following questions: What is the magnitude of the horizontal separation of trajectory endpoints as calculated by several different models? What factors are the major contributors to this separation? Given the limited resolution of the meteorological data upon which the models are based, with what resolution can a trajectory identify a distant source area? We begin in Section 2 by describing the analysis methodology, including a summary of the major features of the trajectory models and the selection criteria for the origins utilized. In Section 3 we present our results, with meteorological analyses of selected cases. A discussion and summary is given in Sections 4 and 5.

2. Methodology

2.1. Description of the trajectory models

Three models were selected for comparison: the Canadian Atmospheric Environment Service 3-dimensional model (AES-3D), and the US National Oceanic and Atmospheric Administration isobaric (NOAA-isobaric) and isentropic (NOAA-isentropic) models. These models were chosen because (a) they are represented in the Arctic haze literature, (b) they are relatively inexpensive to apply, and (c) they are readily available for use by atmospheric transport researchers. A summary of the major features of each model is given in Table 1.

Each model discussed below operates in both the forward (downwind) and backward (upwind) modes; only backward trajectories will be considered in this study. Each model is kinematic in that winds are interpolated directly from gridded analyses without incorporating mass field dynamics. Dynamic models have been applied to atmospheric transport problems (Haagenson and Shapiro, 1979; Merrill et al., 1986), but are not considered in this study because their application has not been reported in the Arctic haze literature. In order to demonstrate the sensitivity of trajectory models to the underlying meteorological data base, additional NOAA-isobaric model runs were performed using gridded analyses from the European Center for Medium-Range Weather Forecasts (ECMWF; Bengtsson et al., 1982).

2.1.1. NOAA-isobaric model. This model is well-established and has been used in conjunction with atmospheric transport problems in both the northern and southern hemispheres. Its major advantage is that the wind field is defined by gridded analyses at mandatory pressure surfaces provided by the US National Meteorological Center (NMC), and is nearly always available (except in cases of gaps in the historical archive).

Table 1. *Major features of the trajectory models used*

Model	Ref.	Meteorological data base	Vertical motion	Model domain
AES-3D	Olson et al. (1978)	CMC gridded analysis	synoptic-scale vertical velocities calculated diagnostically using omega equation	northern hemisphere
NOAA-isobaric	Harris (1982)	NMC gridded analysis	minimal vertical motion: flow follows constant pressure surfaces	global
NOAA-isentropic	Harris and Bodhaine (1983)	NMC gridded analysis	dry adiabatic vertical motion: flow follows surfaces of constant potential temperature	global

Its major disadvantage is that the assumption of isobaric flow is often unrealistic for long-range transport. The severity of this problem may be assessed by running the model at several pressure surfaces and inspecting the level of vertical shear in the horizontal wind.

2.1.2. NOAA-isentropic model. This model represents an improvement over the NOAA-isobaric model by virtue of its ability to diagnose vertical motions. The three-dimensional wind field provided by the NMC gridded analysis is "collapsed" into two dimensions by vertically interpolating the winds to surfaces of constant potential temperature, or isentropes. Dry adiabatic vertical motion is thus implied by the degree of slope in the isentropes. The major advantage of this model is the ability to account for vertical shears as the isentrope samples winds at different altitudes. Its major disadvantage, however, is that isentropic surfaces become undefined in the presence of strong gradients in static stability, such as fronts. The practical consequence of this problem is that isentropic trajectories often terminate prior to the intended length of travel, giving an incomplete description of atmospheric transport.

2.1.3. AES-3D model. This model has the advantage of including orographic and frictional vertical motion, as well as synoptic-scale vertical motion through numerical solution of the omega equation†. Unlike the NOAA-isentropic model, however, the trajectory does not terminate prematurely when it intersects the ground. Instead, advection continues using surface winds until the vertical velocity becomes positive (upward). The model design thus incorporates the effects of vertical shears on horizontal trajectories. The AES-3D model is based on gridded analyses produced by the Canadian Meteorological Center (CMC; Rutherford, 1977; Creswick, 1983).

2.2. Selection criteria for trajectory origins

In order to compare the models described above, it was necessary to select a group of dates and locations to serve as trajectory arrival points, or origins. As the focus of this paper is to compare models which have supported Arctic haze studies, we selected origins corresponding to instrumented aircraft flights conducted during the first and second phases of the Arctic Gas and Aerosol Sampling Program (AGASP-I and -II). AGASP is a multifaceted, cooperative research program designed to determine the distribution, transport, chemistry, aerosol physics, and radiative effects of Arctic haze (Schnell, 1984; Schnell et al., 1989). Intensive field study periods in March–April 1983 and March–April 1986 consisted of airborne measurements tied to similar baseline station measurements at Point Barrow, Alaska (US); Alert, Northwest Territories (Canada); and Ny Alesund, Spitzbergen (Norway).

Origins corresponding to all flights which included vertical soundings of haze constituents were selected. The locations, dates and times are listed in Table 2. Also listed are the corresponding AGASP flight numbers. For further details of the aircraft measurements, refer to Raatz et al. (1985) and Herbert et al. (1987). A total of 31 origins (hereafter referred to as "cases") were selected: 7 during AGASP-I and 24 during AGASP-II. Note that AGASP-II cases correspond to both US and Canadian flights. The origins used are Point Barrow (BRW); Alert (YLT); Bear Island, Norway (BRI); Bodø, Norway (BOD); and the southern Beaufort Sea (BEU).

The cases listed in Table 2 are not meant to comprise a random sample representative of a wide range of meteorological conditions contributing to long-range pollutant transport. Rather, they were selected on the basis of their relation to gas and aerosol measurements constituting a significant portion of what is currently known about Arctic haze. By using these cases for the trajectory model intercomparisons, the relative performance of the models may be evaluated in situations where the haze transport characteristics are reasonably well understood.

2.3. Comparison of trajectory endpoints

The locations of trajectory endpoints for each of the models were compared at 24-h upwind intervals, for a total of 5 days, according to the following procedure. The latitude and longitude of each endpoint were first transformed to fractional grid coordinates on a northern hemi-

† The omega equation gives a diagnostic measure of vertical velocity in terms of the geopotential field (Holton, 1979).

Table 2. *Trajectory origin data*

Case no.	Date	Time (GMT)	Origin	Lat. (°N)	Long. (°)	Flight no.
						AGASP-I:
1	12 Mar 1983	0000	BRW	73.0	157.5 W	1
2	14 Mar 1983	0000	BRW	73.0	157.5 W	2
3	16 Mar 1983	0000	BRW	73.0	157.5 W	3
4	18 Mar 1983	0000	BRW	73.0	157.5 W	4
5	28 Mar 1983	1200	YLT	84.0	62.3 W	7
6	31 Mar 1983	1200	BRI	74.0	25.0 E	8
7	4 Apr 1983	1200	BOD	70.0	12.0 E	9
						AGASP-II:
8	3 Apr 1986	0000	BRW	72.0	158.0 W	US 201
9	7 Apr 1986	1200	YLT	82.5	62.3 W	CAN 10
10	8 Apr 1986	0000	YLT	82.5	62.3 W	CAN 11
11	8 Apr 1986	1200	YLT	82.5	62.3 W	CAN 11
12	8 Apr 1986	1200	BEU	73.5	138.4 W	US 202
13	9 Apr 1986	0000	BEU	73.5	138.4 W	US 202
14	9 Apr 1986	0000	YLT	82.5	62.3 W	CAN 12
15	9 Apr 1986	1200	YLT	82.5	62.3 W	CAN 12
16	10 Apr 1986	0000	BRW	71.0	156.0 W	US 203
17	10 Apr 1986	0000	YLT	82.5	62.3 W	CAN 13
18	10 Apr 1986	1200	YLT	82.5	62.3 W	CAN 13
19	11 Apr 1986	0000	YLT	82.5	62.3 W	CAN 14
20	12 Apr 1986	1200	YLT	82.5	62.3 W	CAN 15
21	13 Apr 1986	0000	YLT	82.5	62.3 W	CAN 16
22	13 Apr 1986	1200	YLT	82.5	62.3 W	US 204
23	14 Apr 1986	0000	YLT	82.5	62.3 W	US 204
24	15 Apr 1986	1200	YLT	82.5	62.3 W	US 206
25	16 Apr 1986	0000	YLT	82.5	62.3 W	US 206
26	17 Apr 1986	1200	YLT	82.5	62.3 W	CAN 18
27	18 Apr 1986	0000	YLT	82.5	62.3 W	CAN 19
28	18 Apr 1986	1200	YLT	82.5	62.3 W	CAN 19
29	19 Apr 1986	0000	YLT	82.5	62.3 W	CAN 19
30	21 Apr 1986	1200	YLT	82.5	62.3 W	CAN 21
31	22 Apr 1986	0000	YLT	82.5	62.3 W	CAN 21

spheric polar stereographic projection. Differences in (I, J) grid indices were converted to horizontal distances $(\Delta x, \Delta y)$ using a mean map scale factor for the two endpoints. Horizontal displacements d were then calculated as $d = [(\Delta x)^2 + (\Delta y)^2]^{1/2}$. In the following sections, average and spread of the displacement distributions will be expressed as median and interquartile range, respectively. Trajectory endpoint displacements 120 h upwind will be referred to as "5-day displacements".

2.4. *Synoptic analyses*

We will show that differences in trajectory calculations among models arise partially from discrepancies in the underlying meteorological data bases. In order to illustrate this, discussions of selected cases in Section 3 will be augmented with synoptic charts based on NMC gridded analyses. We recognize that these discussions are biased toward the synoptic configuration depicted by the NMC data assimilation system (McPherson et al., 1979). However, it is expected that the gross synoptic features analyzed by different data sets are similar. Extensive comparisons of global data sets by Trenberth and Olson (1988) have confirmed this expectation.

3. Results

Trajectories for each case listed in Table 2 were prepared at two levels: 850 mb (~1500 m above msl) and 700 mb (~3000 m above msl), corresponding to levels at which Arctic haze has been commonly encountered aloft (Schnell and Raatz, 1984). Note that while computations by the AES-3D and NOAA-isentropic models begin at 850 or 700 mb, vertical motions diagnosed by these models often result in cross-isobaric transport. Thus transport in these models does not necessarily take place at the original pressure level for the duration of the trajectory.

3.1. 850 mb trajectories

Displacements for 850 mb trajectories are shown in Fig. 1. Analysis at this level has been restricted to a comparison of the AES-3D and NOAA-isobaric models because most of the NOAA-isentropic trajectories terminated prior to 5 days upwind. In Fig. 1, the plotted numbers represent the number of days upwind for which the displacement applies. An asterisk indicates a multiple occurrence (identical or nearly-identical displacements on more than one day). The median 5-day displacement between the AES-3D and NOAA-isobaric models is 1043 km, with an inter-quartile range of 811 km. A consistent relationship between 5-day displacements and trajectory length was not observed.

The major factors contributing to the displacements are the differences in treatments of vertical motions and in the gridded meteorological data bases. The importance of the vertical component

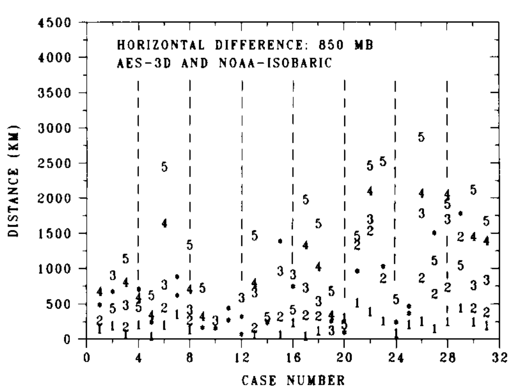

Fig. 1. 850 mb trajectory endpoint displacements (km) between the AES-3D and NOAA-isobaric models. Plotted numbers correspond to the number of days upwind. An asterisk represents multiple occurrences (nearly identical displacements on more than one day).

of long-range atmospheric transport is well-known. Horizontal differences between two- and three-dimensional trajectory models have been shown to be substantial (Artz et al., 1985). Three-dimensional models are thus, in theory, superior to two-dimensional models. However, our results suggest that model sensitivity to the assimilation and analysis procedures producing the meteorological data bases which drive the trajectory models is also quite large.

The effects of driving trajectory calculations with different wind analyses was investigated by running the NOAA-isobaric model using ECMWF gridded analyses. Selected fields from the NMC and ECMWF global analyses have been extensively compared by Trenberth and Olson (1988). They found fairly good overall agreement between area-averaged fields north of the northern hemisphere tropics, although significant local differences in geopotential and wind fields were often noted.

The NMC and ECMWF analyses should, in theory, produce similar trajectories over the time scales considered in this study (5 days). Differences in individual wind values, however, have been shown to cause substantial differences in trajectories (Kahl and Samson, 1988b). Although it is not possible in the present study to quantify the effects of different data bases relative to different vertical motion parameterizations, some insight can be gained by inspecting individual cases in more detail. Case nos. 6, 22, 23 and 26 (see Fig. 1) represent the highest 10% of the 5-day displacement distribution, with values greater than 2460 km. In the following paragraphs, we analyze two of these cases (nos. 6 and 22) in detail.

Trajectories and synoptic analyses corresponding to case no. 6, arriving at Bear Island, Norway at 1200 GMT on 31 March 1983, are shown in Fig. 2. At this time a weak high pressure ridge at 850 mb covered the Norwegian Sea, and a weak low pressure system was located over the eastern Barents Sea. Bear Island was directly between these two systems in a region of light easterly winds. The AES-3D model showed a slight northerly component, while the NOAA-isobaric model showed a slight southerly component. Two days earlier, on 29 March, the trajectories were located in the Barents Sea. At this time the winds had increased due to the formation of high pressure in

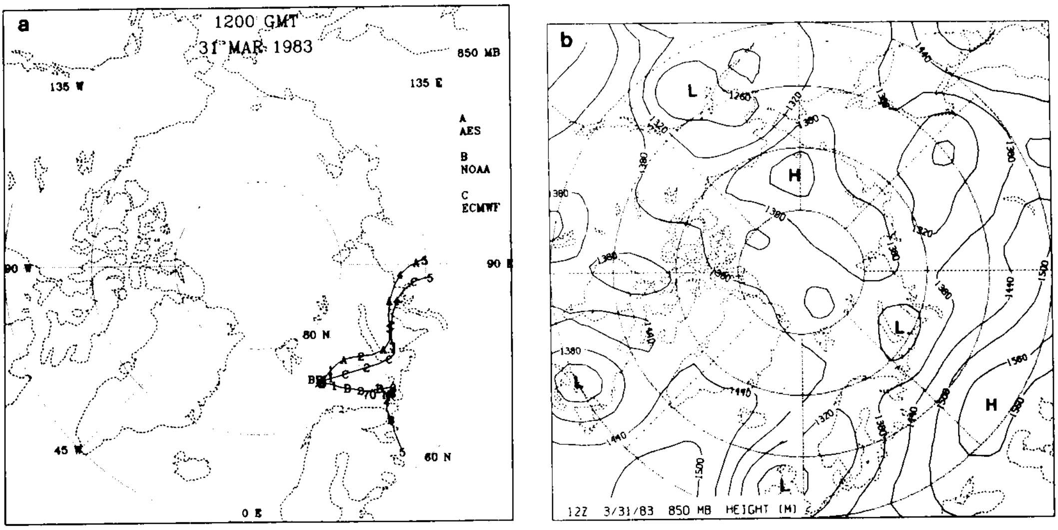

Fig. 2. (a) 850 mb trajectories corresponding to case no. 6. Plotted numbers indicate the number of days upwind; (b) 850 mb synoptic analysis (geopotential height, m) for 1200 GMT on 31 March 1983.

the Kara Sea and a weak low pressure system in the Ukraine. To the west, a deep low pressure system had formed over Iceland. Winds over the Barents Sea were southeasterly. The large increase in the separation between endpoints beyond 3 days upwind results from the two tracks coming under the influence of separate low pressure systems. The AES-3D trajectory shows a northerly track on the back side of a low in the central USSR. The NOAA-isobaric trajectory is to the south in response to a low centered over western Norway.

The 850 mb trajectories shown in Fig. 2a include NOAA-isobaric model calculations using the ECMWF data base (line C). Despite its lack of vertical motion, the path of this trajectory is similar to the AES-3D model path. The AES-3D model exhibited only a small amount of vertical motion (maximum cumulative oscillation of 500 m in 5 days). The similarity of the NOAA-isobaric trajectory using ECMWF data with the AES-3D trajectory, and the limited vertical motion of the AES-3D trajectory, indicates that the large 5-day displacement (2460 km) between the AES-3D and NOAA-isobaric models (lines A and B) is primarily due to differences in the meteorological analyses.

Trajectories and synoptic analyses corresponding to case no. 22, arriving at Alert at 1200 GMT on 13 April 1986, are shown in Fig. 3. In this case the discrepancy between the AES-3D and NOAA-isobaric models is clearly determined in the first 24 h. On 13 April the NMC 850 mb analysis showed a low pressure trough extending from the pole to Ellesmere Island, with a ridge positioned over Greenland (Fig. 3c). The NOAA-isobaric trajectory (Fig. 3a) followed the southerly winds around the ridge for the first 2 days upwind. The CMC analysis apparently positioned the ridge further to the west, causing the AES-3D trajectory to exhibit southwesterly, then westerly flow. At 5 days upwind, the trajectory endpoints were separated by 2500 km.

NOAA-isobaric trajectories at three pressure levels are shown in Fig. 3b. These trajectories traverse similar paths for the first few days upwind, with the lowest level (1000 mb) track following weaker winds than the upper levels. The small amount of vertical wind directional shear during the first 48 h upwind of Alert provides additional evidence that differences in the NMC and CMC analyses were in large part responsible for the large displacements in this case.

Case nos. 1, 2, 4, 10, 12, 14 and 20 represent the lowest 25% of the 5-day displacement distribution, with values less than 500 km. Trajectories for case no. 1, a representative example from this

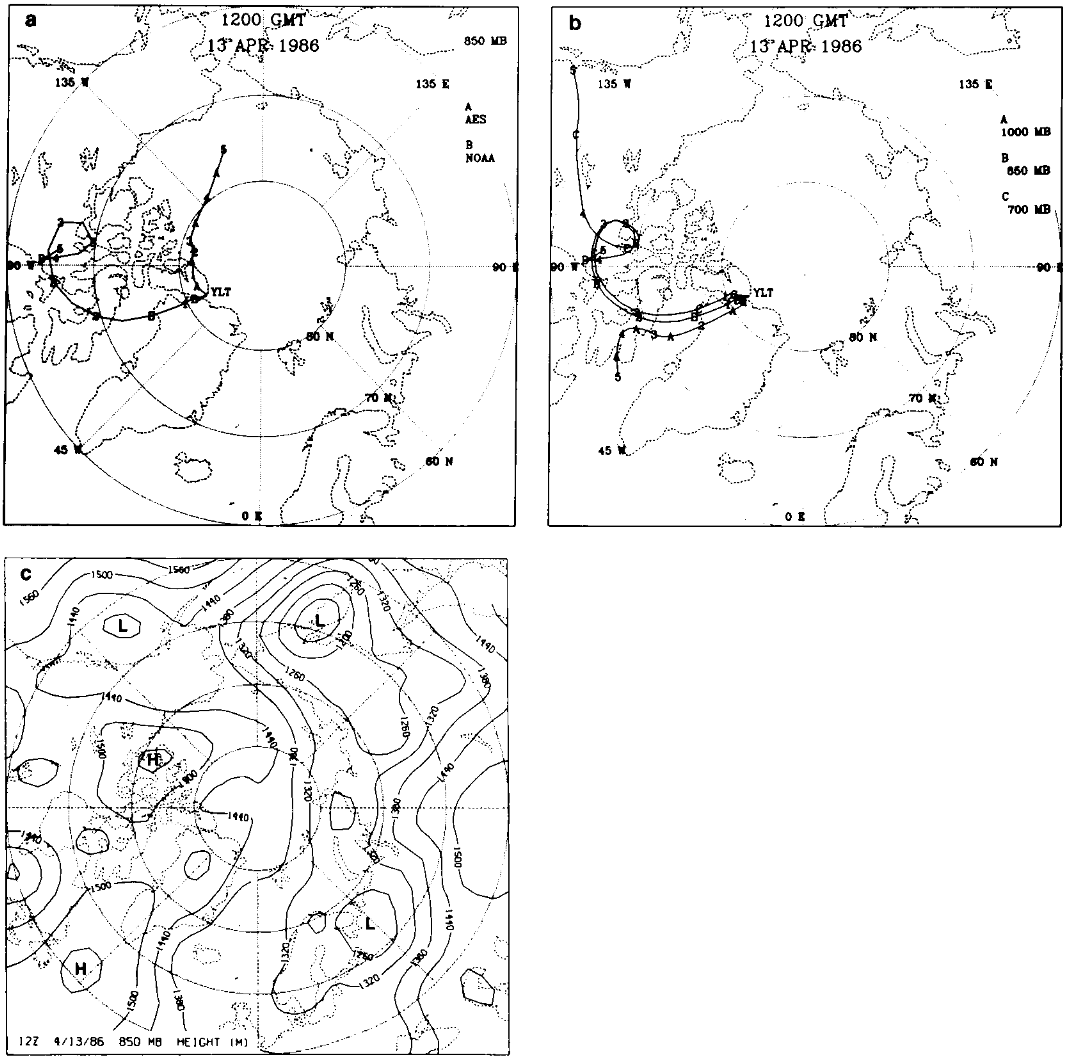

Fig. 3. (a) 850 mb trajectories corresponding to case no. 22; (b) NOAA-isobaric trajectories for case no. 22 at three pressure levels; (c) 850 mb synoptic analysis (geopotential height, m) for 1200 GMT on 13 April 1986.

group, are shown in Fig. 4. 850 mb trajectories from the AES-3D and NOAA-isobaric models (Fig. 4a) and NOAA-isobaric trajectories at several pressure levels (Fig. 4b) all follow an anticyclonic path around a deep high pressure center in the East Siberian Sea. AES-3D trajectories at other levels (not shown) also followed this path. Very little directional shear is evident in the wind field (Fig. 4b), although the lowest-level trajectory (1000 mb) sampled slower wind speeds compared to the higher levels. The AES-3D 850 mb trajectory exhibited a vertical oscillation of 503 m (maximum–minimum altitude along trajectory). Note that although the 5-day displacement was almost 500 km, the path, speed and curvature of the trajectories are nearly identical. This implies that over the distance scales considered here (the NOAA-isobaric trajectory traveled over 5000 km), the trajectories are nearly equivalent, at least for the purpose of identifying an upwind source region.

The following common characteristics were observed for trajectories in the lowest 25% of the 5-day displacement distribution: (1) There was

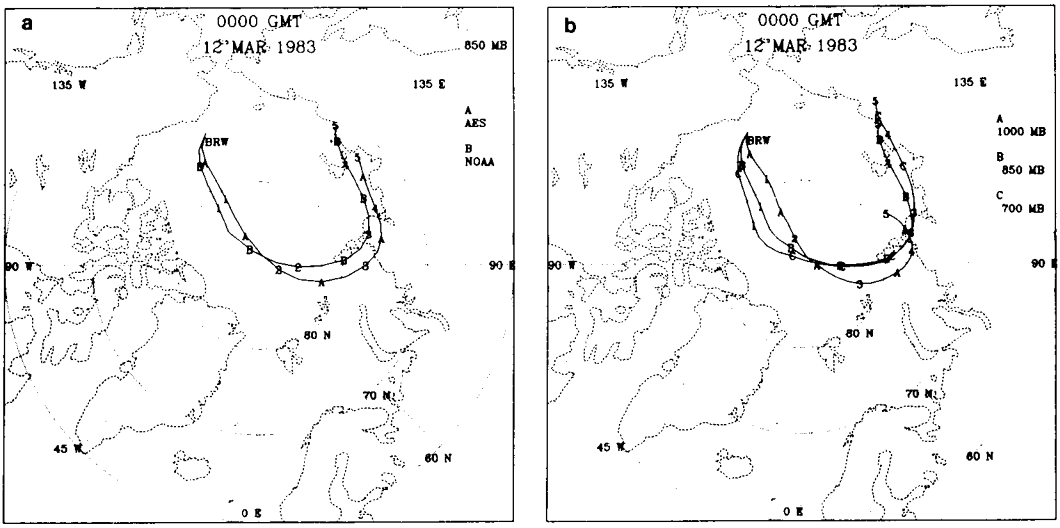

Fig. 4. (a) 850 mb trajectories corresponding to case no. 1; (b) NOAA-isobaric trajectories for case no. 1 at three pressure levels.

little shear between 850 and 700 mb NOAA-isobaric trajectories; (2) vertical oscillations in the AES-3D trajectories ranged from 300–1200 m; and (3) 5-day displacements were less than 500 km. During these cases the relative lack of vertical shear prevented the vertical velocities in the AES-3D model from giving significantly different transport estimates from the NOAA-isobaric model. In each of these cases trajectories from both models exhibited similar curvature and speed, suggesting that the analyzed wind flow in both gridded data bases were similar.

3.2. 700 mb trajectories

Comparison of 700 mb trajectories was restricted to those cases for which calculations for all three models extended back to 5 days upwind. Premature termination of NOAA-isentropic trajectories forced the elimination of 17 cases, leaving 14 cases for analysis. Of the 17 cases eliminated, 13 were due to the intersection of the isentropic surface with the ground. The remaining 4 cases terminated prematurely due to gaps in selected fields in the NMC data archive.

Displacements for 700 mb trajectories are shown in Fig. 5. Median 5-day displacements in km (with inter-quartile ranges in parentheses) between AES-3D and NOAA-isobaric; AES-3D and NOAA-isentropic; and NOAA-isobaric and NOAA-isentropic trajectories were 825 (1651); 1016 (1669); and 321 (440), respectively. 5-day displacements between models were generally in the 500–2000 km range. 5-day displacements between the AES-3D and each of the NOAA models for cases 26, 27 and 28, however, were substantially larger. One of these cases (no. 28) will be discussed further below.

As shown in Fig. 5, differences between NOAA-isobaric and NOAA-isentropic trajectories (Fig. 5c) were mostly <1000 km. These values are smaller than differences between AES-3D and either of the NOAA models (Figs. 5a, b). This arises from the relatively low levels of vertical wind shear in the 14 cases utilized for the 700 mb comparisons. Inspection of plots of NOAA-isobaric trajectories at several pressure levels, such as in Figs. 3b and 4b, revealed relatively little shear along the trajectories, particularly between the 850 and 700 mb levels. As it is well-known that vertical shears cause large differences between isobaric and isentropic trajectory models (e.g., Artz et al., 1985), these 14 cases represent an opportunity to study trajectory models during situations in which model sensitivity to the meteorological data base is likely to contribute a large portion of the total sensitivity.

Differences between the AES-3D model and the NOAA-isentropic model are due to both (a) differences in parameterizations of vertical motions (synoptic vertical velocities versus adia-

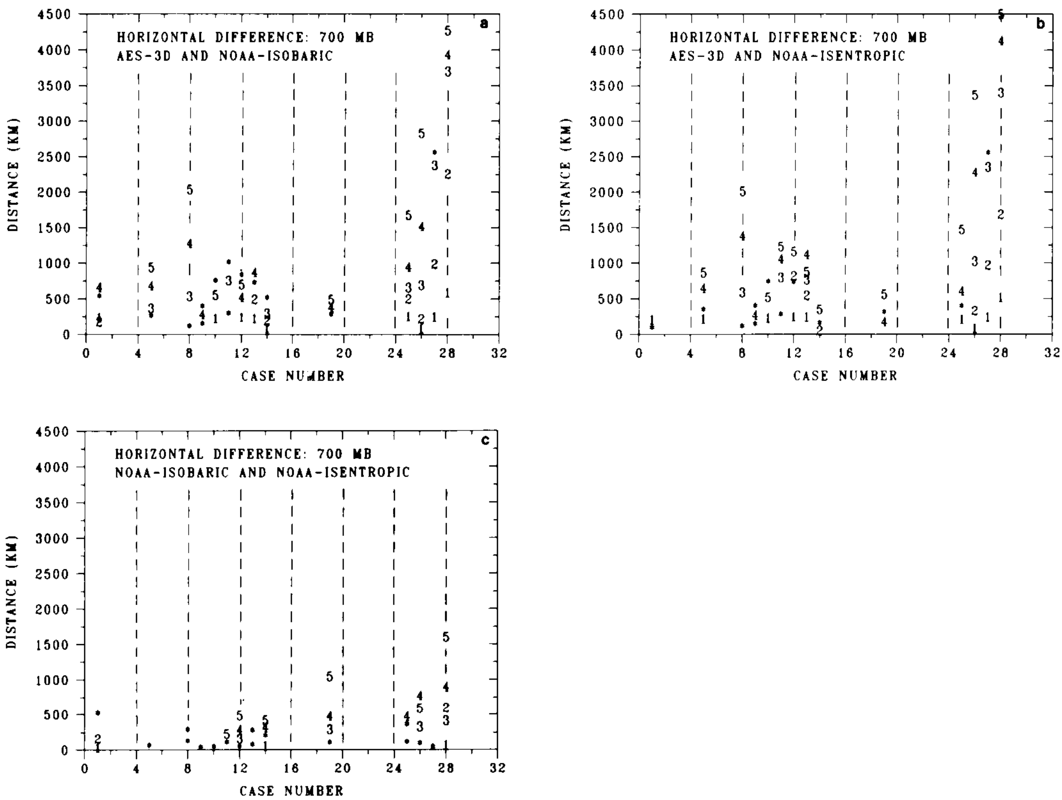

Fig. 5. 700 mb trajectory endpoint displacements as in Fig. 1: (a) AES-3D and NOAA-isobaric models; (b) AES-3D and NOAA-isentropic models; (c) NOAA-isobaric and NOAA-isentropic models.

batic flow), and (b) differences in the CMC and NMC gridded data. In the Arctic winter and spring one would expect the vertical motion parameterizations to be approximately equivalent, particularly for 700 mb trajectories which are detached from diabatic boundary-layer forcing. 5-day displacements between these models were considerably larger than those between the NOAA models. Assuming that the vertical motion parameterizations are approximately equivalent, this suggests that differences between the CMC and NMC data bases were responsible for a large portion of differences between these models.

The result that differences between the AES-3D and NOAA-isobaric models were similar to differences between the AES-3D and NOAA-isentropic models lends support to the hypothesis that differences in the CMC and NMC data bases are responsible for a large portion of the observed differences in 700 mb trajectories. In addition to the different data bases used, the AES-3D and NOAA-isobaric models differ in that the former model includes the effects of synoptic vertical velocities, while the latter model assumes purely isobaric flow. It follows that displacements between these models would be expected to be larger than those between the AES-3D and NOAA-isentropic models due to the combined sensitivity to both of these factors. The similarity in differences between the AES-3D and *either* of the NOAA models indicates that for the 14 cases considered here, trajectory model sensitivity to the gridded meteorological fields is a substantial component of the endpoint displacements.

In order to further demonstrate the sensitivity of trajectory models to the meteorological data base, the NOAA-isobaric model was run using the ECMWF gridded analyses. Comparison of

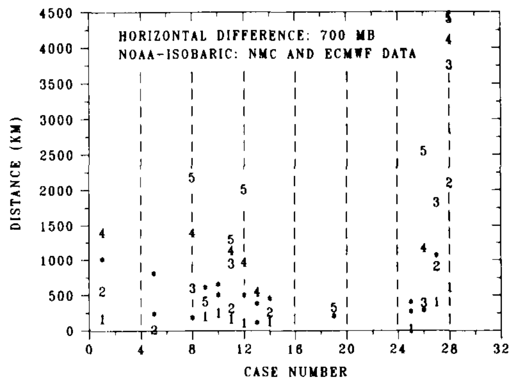

Fig. 6. 700 mb trajectory endpoint displacements as in Fig. 1: NOAA-isobaric models based on NMC and ECMWF gridded meteorological analyses.

these trajectories with NOAA-isobaric trajectories based on NMC data are shown in Fig. 6. The magnitude of these displacements closely resemble those of displacements between the AES-3D and NOAA models (Figs. 5a and b). While the results shown in Fig. 6 represent trajectory model sensitivity to the meteorological data base only, those in Figs. 5a, b represent sensitivity to both the data base *and* model parameterizations. Comparison of these figures again demonstrates that, for the cases considered in this study, the disparity in trajectory calculations due to differences in the underlying meteorological data base is at least as great as that due to differences in model parameterizations of vertical motion.

A striking example of the effects of different data sets is shown in Fig. 7. Fig. 7a shows 700 mb trajectories arriving at Alert (case no. 28), along with a 700 mb synoptic analysis (Fig. 7b) for 0000 GMT on 18 April 1986. The NOAA models based on NMC data (lines B and C) traversed nearly identical paths for the first 3 days upwind. At 5 days upwind the endpoints were separated by nearly 1600 km, due to differential vertical motions between the two models. The flow for these models was primarily influenced by a high pressure system located in the central polar basin, extending across the pole into the Greenland and Norwegian seas. The AES-3D model (line A) and NOAA-isobaric model based on ECMWF data (line D) followed an entirely different path. These trajectories were nearly identical, following a cyclonic path around a low-pressure system centered over Baffin Bay. At 5 days the NOAA-isobaric trajectories based on NMC and ECMWF data (lines B and D) were separated by 4500 km. This example illustrates the potential for gross disparity in trajectories based on differences in gridded meteorological analyses.

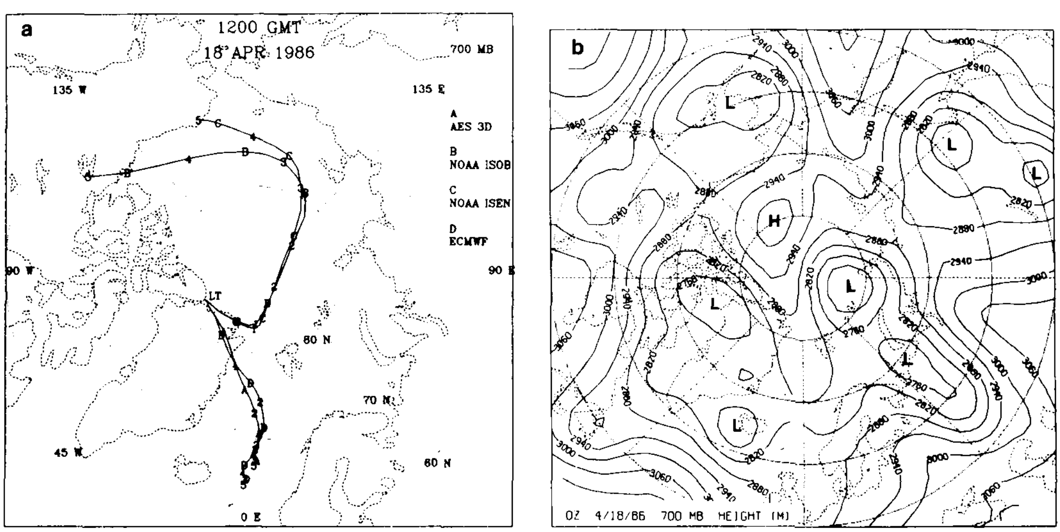

Fig. 7. (a) 700 mb trajectories corresponding to case no. 28; (b) 700 mb synoptic analysis (geopotential height, m) for 0000 GMT on 18 April 1986.

4. Discussion

The results presented above illustrate the sensitivity of trajectory models to differences in the underlying meteorological data bases. This study does not address trajectory errors. However, a comparison of the present study with previous research on trajectory errors is helpful to put the sensitivity results into proper perspective.

Extrapolation of Kuo et al. (1985) and Kahl and Samsons' (1986; 1988a) evaluations of trajectory model uncertainties suggests that 5-day horizontal errors of 500–800 km should be expected. These errors are a result of spatial and temporal interpolation of meteorological measurements, primarily rawinsondes, on the synoptic scale. In the Arctic, where there are few in situ measurements, it is reasonable to expect errors of up to 800 km after 5 days. The median 5-day displacements shown in Figs. 1, 5 and 6 are in the 800–1000 km range, with the exception of differences between the 700 mb NOAA trajectories. In general, then, the median 5-day displacements are approximately in accordance with the expected uncertainties arising from the interpolation process.

Given these uncertainties, the resolution of long-range trajectory models for purposes of upwind source determination is limited to the identification of areal source regions with fairly broad dimensions. Based on the model intercomparisons presented here, a conservative estimate of these dimensions is $\sim$1000 km. This estimate would also apply to forward (downwind) trajectories, i.e., the resolution with which a downwind impact area may be identified is approximately 1000 km.

In cases with 5-day displacements between models greater than about 1000 km, the use of individual trajectories to diagnose atmospheric transport has exceeded the precision of the models. These large displacements indicate the presence of complicating factors such as differential horizontal advection by large vertical shears, and the possibility of significant differences in the meteorological data bases used.

Because atmospheric transport researchers generally do not have several models and several data bases at their disposal, it is usually impractical (if not impossible!) to evaluate the precision of trajectory calculations in individual cases. An indication of the representativeness of individual trajectories may be obtained, however, by the method described by Merrill et al. (1985). This method involves the calculation of trajectories at 1° latitude increments (111.1 km) on a rectangular area 3° or 4° on a side centered at the trajectory origin. The resulting trajectory ensemble depicts the transport characteristics of a 10^5 km^2 area, and enables an assessment of the spatial homogeneity of the flow. The outer boundaries defined by the ensemble should serve to identify the range of possible upwind or downwind source regions, as well as to determine whether the trajectories encounter deformation zones where widely divergent solutions are possible.

This technique was applied using rectangular arrays of nine 850 mb NOAA-isobaric trajectories at 111 km increments. The ensemble shown in Fig. 8 corresponds to case no. 6. This case was in the top 10% of the 5-day displacement distribution, with a separation of 2460 km. The divergence in endpoints suggests that the trajectories are of questionable value beyond 3 days upwind. Comparison of this figure with Fig. 2a confirms that, in this case, the contrasting transport scenarios given by different models could have been anticipated by applying the ensemble method with a single model.

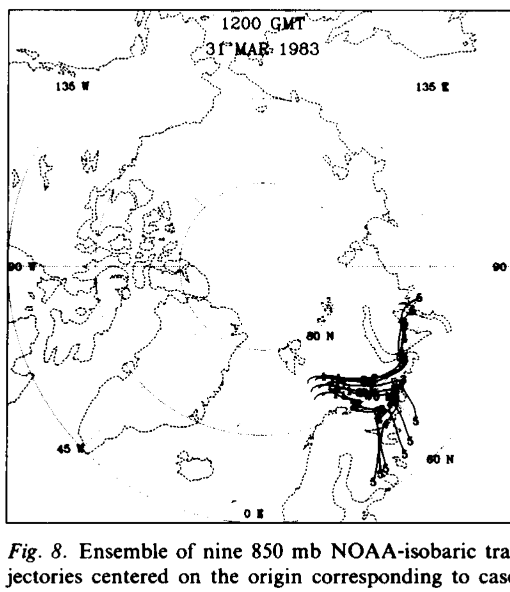

Fig. 8. Ensemble of nine 850 mb NOAA-isobaric trajectories centered on the origin corresponding to case no. 6. Origin points are separated by 111 km.

A trajectory ensemble corresponding to case no. 1 is shown in Fig. 9. This case was among the lowest 25% of the 5-day displacement distribution, with a value under 500 km. The ensemble shows that the flow is spatially homogeneous for the duration of the trajectory. As borne out by the model comparison shown in Fig. 4a, the coherence of the ensemble suggests that in this case, an individual trajectory is likely to be representative of the mean transport over a 5-day period. Examination of ensembles for other extreme (large and small displacements) cases revealed a consistent correlation between the divergence of trajectories within ensembles and 5-day displacement values between models.

The ensemble method is not expected to give a clear indication of the representativeness of trajectories in all cases. As demonstrated above, however, it is a useful tool in certain situations. As noted earlier, trajectories incorporating vertical motion should theoretically give a more coherent picture of long-range atmospheric transport. This is especially true in baroclinic transport events in which neglect of vertical shears could result in incorrect attribution of distant source regions. In practice, however, the limitations imposed by interpolating available meteorological data bases make it difficult to distinguish additional vertical "signals" from the "noise" of interpolation uncertainties. The best compromise is to use a model incorporating vertical motion in conjunction with the ensemble method described above.

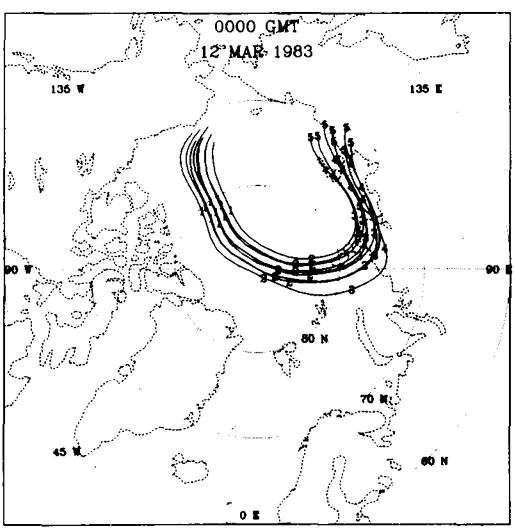

Fig. 9. As in Fig. 8, but for case no. 1.

5. Summary and concluding remarks

A comparison of three long-range trajectory models for selected cases corresponding to Arctic haze measurements has revealed the following.

(i) Median differences between 5-day trajectory endpoints ranged from 800–1000 km. However, differences between the NOAA-isobaric and NOAA-isentropic models were substantially smaller due to reduced levels of wind shear in the cases selected.

(ii) The sensitivity of trajectory models to differences in the gridded meteorological data bases is substantial, and can be greater than the sensitivity to differences in parameterizations of vertical motion.

(iii) Given the uncertainties in long-range trajectory models, their usefulness after 5 days is limited to the identification of source regions with horizontal dimensions on the order of 1000 km.

When applied cautiously, trajectory analysis remains a powerful tool for determining the pathways and source regions of airborne material. Certain steps should be taken to assess the representativeness of individual trajectories. For example, trajectories at different vertical levels should be inspected to assess vertical shears. The presence of large shears implies a complicated transport event which may not be well-represented by a single trajectory. In addition, Merrill et al.'s (1985) ensemble technique is recommended. Assessment of the spatial homogeneity of the ensemble flow pattern provides an indication of the representativeness of individual trajectories in evaluating long-range transport.

6. Acknowledgements

This research was performed while J. Kahl was a National Research Council Research Associate at NOAA's Geophysical Monitoring for Climatic Change laboratory. The ECMWF fields used in this study were provided to NOAA/GMCC by the Director, European Center for Medium-Range Weather Forecasts, Reading, Berkshire, UK.

REFERENCES

Artz, R., Pielke, R. A. and Galloway, J. 1985. Comparison of the ARL/ATAD constant level and the NCAR isentropic trajectory analyses for selected case studies. *Atmos. Environ. 19*, 47–63.

Bengtsson, L., Kanamitsu, M., Kållberg, P. and Uppala, S. 1982. FGGE 4-dimensional data assimilation at ECMWF. *Bull. Am. Meteorol. Soc. 63*, 29–43.

Carlson, T. N. 1981. Speculations on the movement of polluted air to the Arctic. *Atmos. Env. 8*, 1473–1478.

Creswick, W. S. 1983. Objective analysis at the CMC. CMC Information, *Vol. 1, No. 3*, Canadian Meteorological Centre, Dorval, Quebec, pp. 22–39.

Draxler, R. R. 1987. Sensitivity of a trajectory model to the spatial and temporal resolution of the meteorological data during CAPTEX. *J. Climate Appl. Meteor. 26*, 1577–1588.

Haagenson, P. and Shapiro, M. A. 1979. Isentropic trajectories for derivation of objectively analyzed meteorological parameters. NCAR Tech. Memo. *NCAR/TN-149 + STR*, 30 pp.

Haagenson, P. L., Kuo, Y.-H., Skumanich, M. and Seaman, N. L. 1987. Tracer verification of trajectory models. *J. Climate Appl. Meteor. 26*, 410–426.

Harris, J. M. 1982. The GMCC atmospheric trajectory program. NOAA Tech. Memo. *ERL ARL-116*, Air Resources Laboratory, Silver Spring, MD, 30 pp.

Harris, J. M. and Bodhaine, B. A.(eds.) 1983. Geophysical Monitoring for Climatic Change, *No. 11*, Summary Report 1982. Environmental Research Laboratory, Boulder, CO, 160 pp.

Herbert, G. A., Bridgman, H. A., Schnell, R. C., Bodhaine, B. A. and Oltmans, S. J. 1987. The analysis of meteorological conditions and haze distribution for the second Arctic gas and aerosol sampling program (AGASP II), March–April 1986. NOAA Tech. Memo. *ERL ARL-158*, Air Resources Laboratory, Silver Spring, MD, 67 pp.

Holton, J. R. 1979. *An introduction to dynamic meteorology*. New York: Academic Press, 391 pp.

Iversen, T. 1984. On the atmospheric transport of pollution to the Arctic. *Geophys. Res. Lett. 11*, 457–460.

Kahl, J. D. and Samson, P. J. 1986. Uncertainty in trajectory calculations due to low resolution meteorological data. *J. Climate Appl. Meteor. 25*, 1816–1831.

Kahl, J. D. and Samson, P. J. 1988a. Uncertainty in estimating boundary-layer transport during highly convective conditions. *J. Appl. Meteor. 27*, 1024–1035.

Kahl, J. D. and Samson, P. J. 1988b. Trajectory sensitivity to rawinsonde data resolution. *Atmos. Environ. 22*, 1291–1299.

Kuo, Y.-H., Skumanich, M., Haagenson, P. L. and Chang, J. S. 1985. The accuracy of trajectory models as revealed by the observing system simulation experiments. *Mon. Wea. Rev. 113*, 1852–1867.

McPherson, R. D., Bergman, K. H., Kistler, R. E., Rasch, G. E. and Gordon, D. S. 1979. The NMC operational global data assimilation system. *Mon. Wea. Rev. 107*, 1445–1461.

Merrill, J. T., Bleck, R. and Avila, L. 1985. Modeling atmospheric transport to the Marshall Islands. *J. Geophys. Res. 90*, 12927–12936.

Merrill, J. T., Bleck, R. and Boudra, D. 1986. Techniques of lagrangian trajectory analysis in isentropic coordinates. *Mon. Wea. Rev. 114*, 571–581.

Mitchell, J. M., Jr. 1957. Visual range in the polar regions with particular reference to the Alaskan Arctic. *J. Atmos. Terr. Phys. Spec. Suppl. Pt. 1*, 195–211.

Olson, M. P., Oikawa, K. K. and Macafee, A. W. 1978. A trajectory model applied to the long-range transport of air pollutants: a technical description and some model intercomparisons. Tech. Rep. *LRTAP 78-4*, Air Quality and Inter-Environmental Research Branch, Atmospheric Environment Service, Downsview, Ontario.

Raatz, W. E., Schnell, R. C. and Bodhaine, B. A. 1985. Atmospheric cross sections for the Arctic gas and aerosol sampling program, March–April 1983. NOAA Tech. Memo. *ERL ARL-134*, Air Resources Laboratory, Silver Spring, MD, 50 pp.

Reiff, J., Forbes, G. S., Spieksma, F. Th. M. and Reynders, J. J. 1986. African dust reaching northwestern Europe: a case study to verify trajectory calculations. *J. Climate Appl. Meteor. 25*, 1543–1567.

Rutherford, I. D. 1977. An operational three-dimensional multi-variate statistical objective analysis scheme. Scientific Notes, RPN, *No. 1*, Atmospheric Environment Service, Dorval, Quebec.

Schnell, R. C. 1984. Arctic haze and the Arctic Gas and Aerosol Sampling Program (AGASP). *Geophys. Res. Lett. 11*, 361–364.

Schnell, R. C. and Raatz, W. E. 1984. Vertical and horizontal characteristics of Arctic haze during AGASP: Alaskan Arctic. *Geophys. Res. Lett. 11*, 369–372.

Schnell, R. C., Watson, T. B. and Bodhaine, B. A. 1989. NOAA WP-3D instrumentation and flight operations on AGASP-II. *J. Atmos. Chem.*, in press.

Trenberth, K. E. and Olson, J. G. 1988. An evaluation and intercomparison of global analyses from the National Meteorological Center and the European Centre for Medium Range Weather Forecasts. *Bull. Am. Meteorol. Soc. 69*, 1047–1057.